Structure and Function

1

The diagnosis of skin disease is based on color, morphology, and distribution of cutaneous lesions. The structure of the skin and associated appendages relates directly to these characteristics.

Folliculitis presents with papules or pustules. Follicular accentuation is characteristic of any eruption in darker-skinned races. In patients with miliaria, involvement of the sweat gland ostia results in erythematous papules, pustules, or superficial vesicles in areas of heavy sweating. The vesicles of miliaria crystallina are irregular in shape because the stratum corneum fails to impede the spread of the blister in random directions. This is in stark contrast to spongiotic and subepidermal blisters, which are distinctly round—as in acute dyshidrotic eczema or bullous pemphigoid.

The color of a cutaneous eruption relates to various pigments. Brown pigments include melanin, lipofuscin, and hemosiderin. Brown pigments located deeper in the dermis impart a blue hue because of diffraction of light. This is evident in blue nevi as a result of deep melanin and as a result of lipofuscin present in the sweat within nodular hidradenomas. Red pigment relates to oxygenated hemoglobin and blue to deoxygenated hemoglobin. Dilatation or proliferation of blood vessels and the rapidity of blood flow produce various shades of red and blue. Yellow pigments relate to lipid deposition or carotenoids dissolved in the cytoplasm of epithelial cells and histiocytes. In granulomatous disease, diascopy removes the visible appearance of oxygenated hemoglobin, allowing the observer to see the apple jelly yellow appearance of carotenoids within the cytoplasm. This section of the atlas will focus on the structure of the skin and how that structure translates to clinical manifestations of disease.

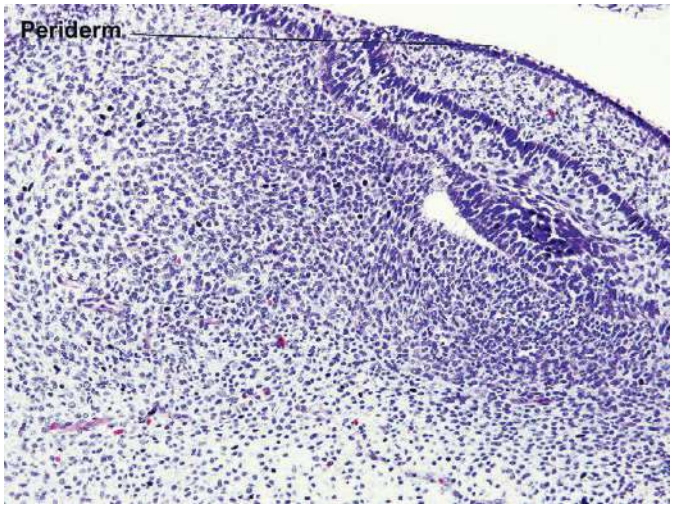

Fig. 1.1 In early fetal life, a cuboidal periderm is present rather than an epidermis. Fetal skin, H&E × 40.

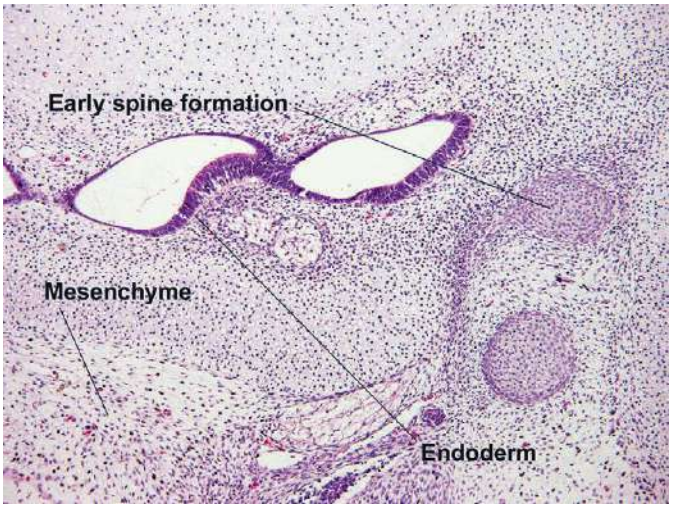

Fig. 1.2 In early fetal life, the spine is composed of cartilage, and mesenchyme is present rather than a dermis. Mesenchyme heals without scar formation. Once dermis forms, scars will occur after injury. Fetal skin, H&E × 40.

Fig. 1.3 Skin in young children is characterized by small adnexal structures and fine dermal collagen bundles that stain deep red in contrast to the thick, pink collagen bundles of an adult. Many plump fibroblasts are present in the dermis, actively synthesizing collagen. Childhood skin, H&E × 20.

Fig. 1.4 Facial skin is characterized by prominent sebaceous follicles, often containing *Demodex* mites. Facial skin, H&E × 40.

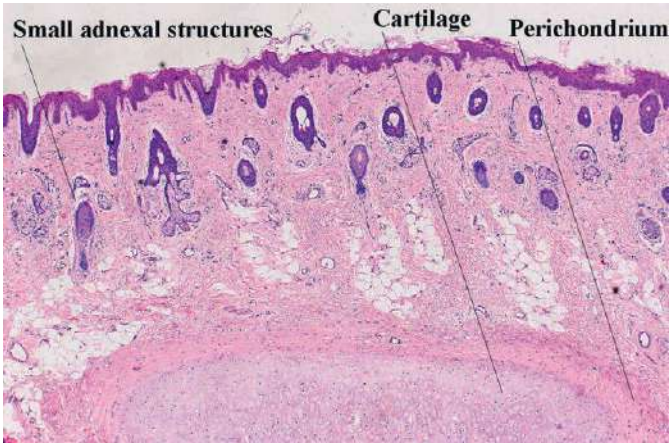

Fig. 1.5 Skin of the ear demonstrates small adnexal structures with an elastic cartilage surrounded by a red perichondrium. Ear skin, H&E × 20.

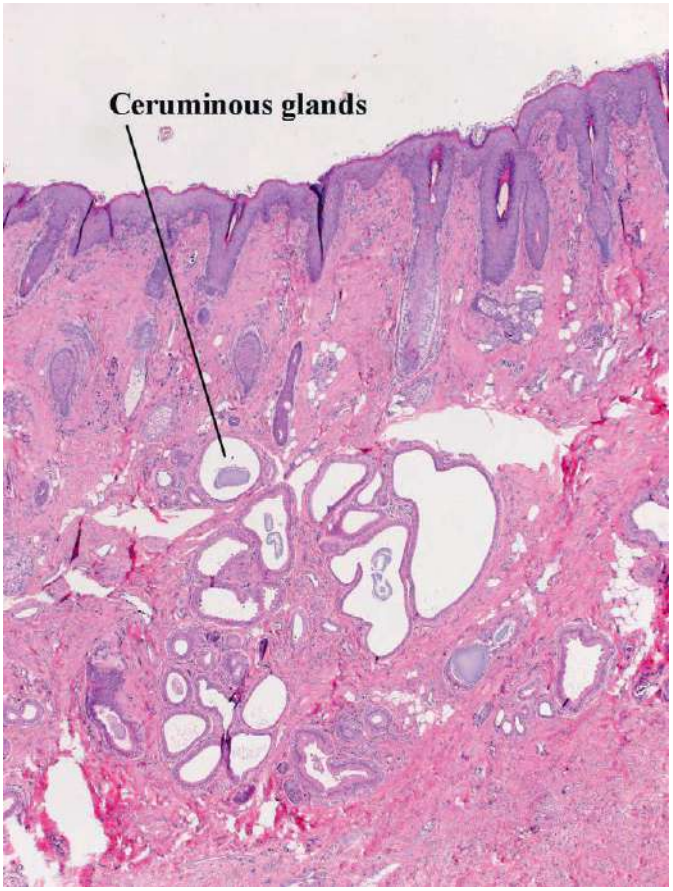

Fig. 1.6 The structure of the ear canal is similar to other parts of the ear, except for the presence of ceruminous glands, which represent modified apocrine glands. Ear canal skin, H&E × 20.

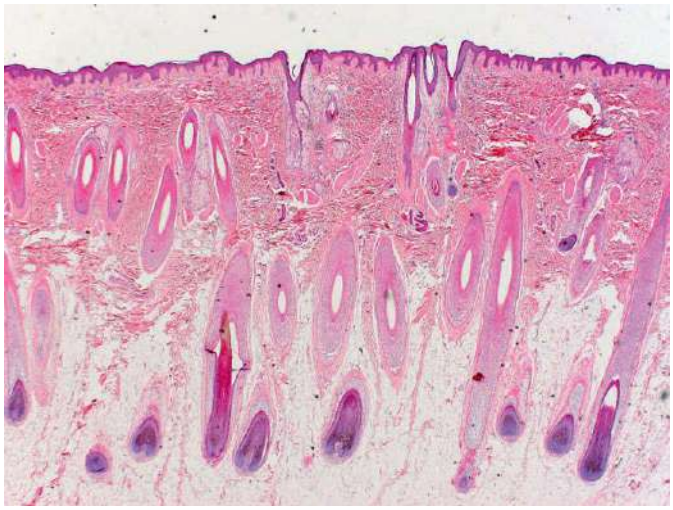

Fig. 1.7 Scalp skin demonstrates many terminal hair follicles. The inferior segment of each follicle sits within the subcutaneous fat. Scalp skin, H&E × 40.

Fig. 1.8 Axillary skin is rugose and demonstrates large apocrine glands. Axillary skin, H&E × 40.

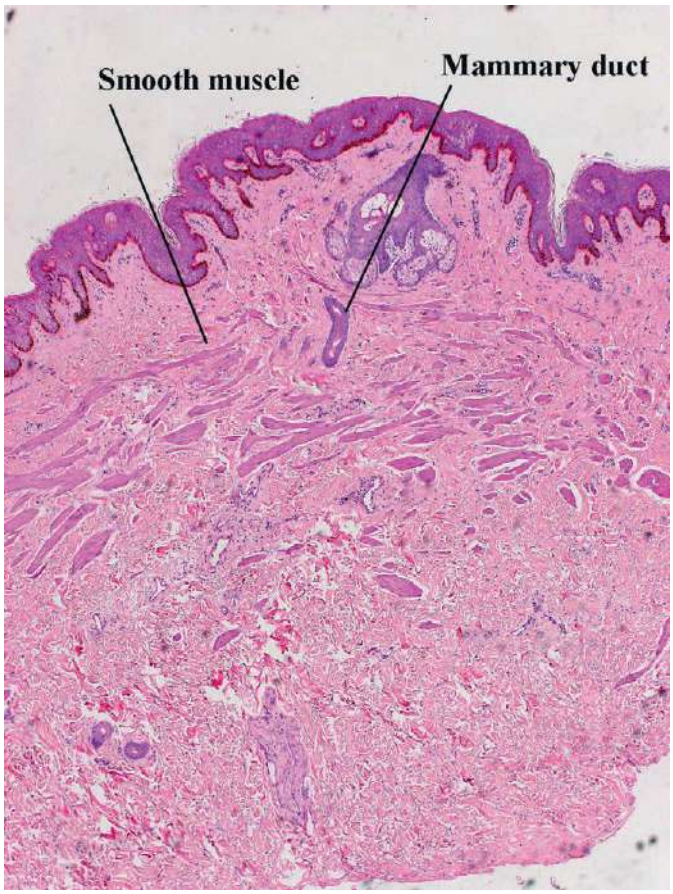

Fig. 1.9 Breast skin demonstrates numerous smooth muscle bundles. Breast skin, H&E × 20.

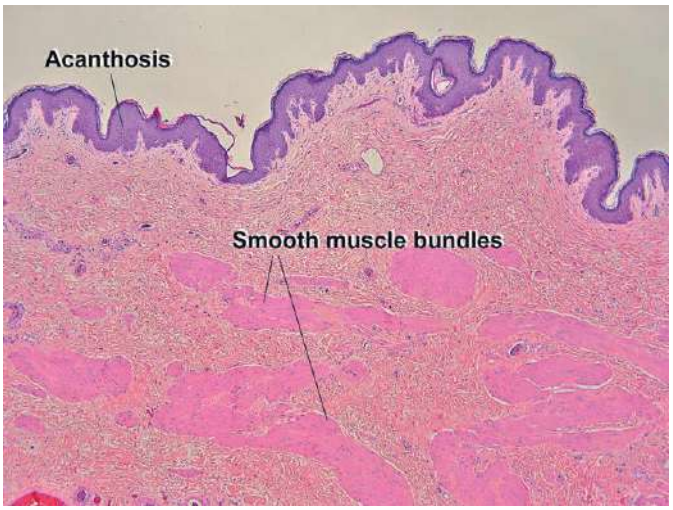

Fig. 1.10 Nipple skin demonstrates smaller smooth muscle bundles. The mammary duct resembles a large sweat duct. Breast skin, H&E × 20.

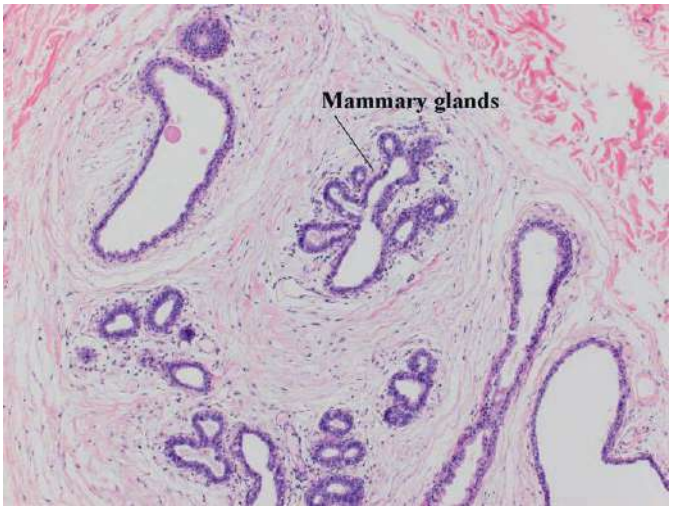

Fig. 1.11 The secretory portion of mammary glands demonstrates columnar epithelium forming complex lumens. Breast skin, H&E × 100.

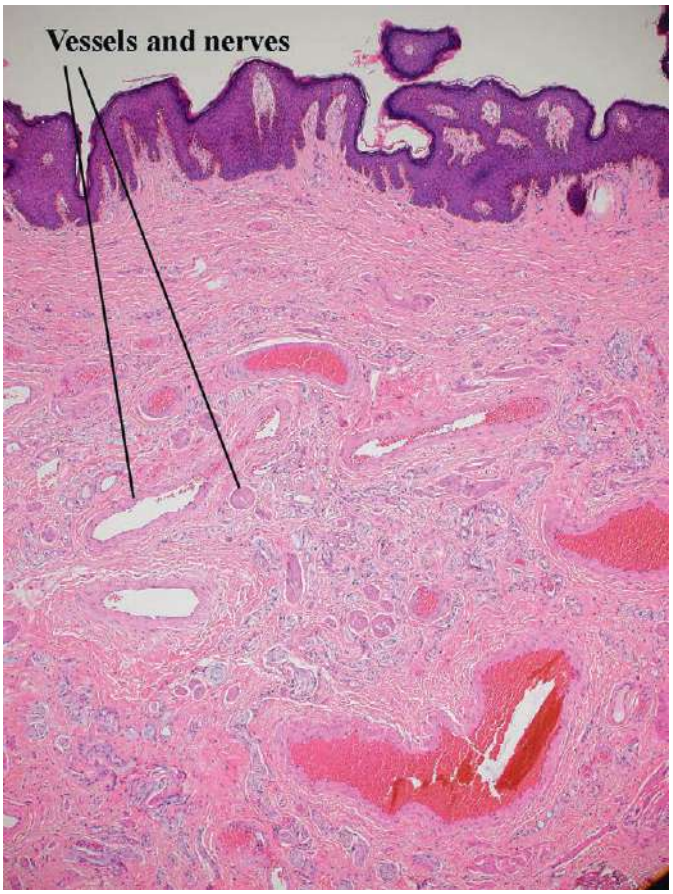

Fig. 1.12 Prepuce demonstrates a rugose appearance with many smooth muscle fascicles and high vascularity. Prepuce, H&E × 20.

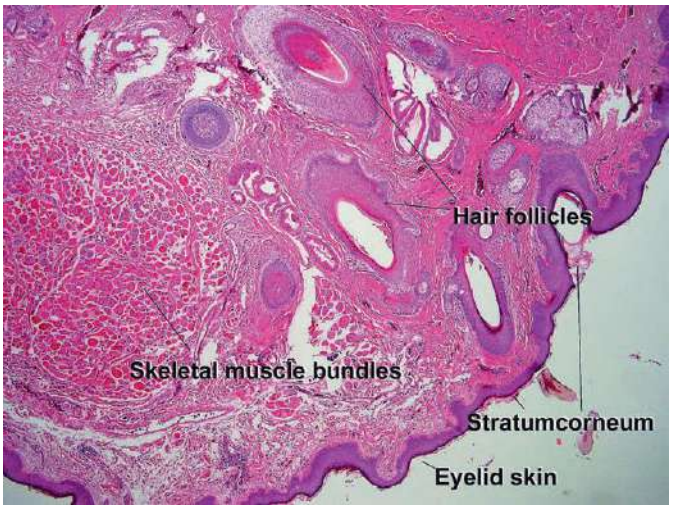

Fig. 1.14 The lid margin; on the cutaneous surface of the lid, a layer of striated muscle is present below the epidermis, H&E × 10.

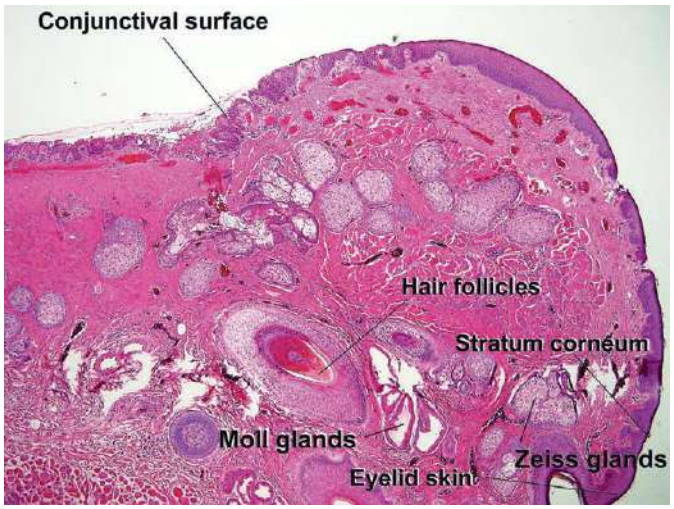

Fig. 1.13 Eyelid anatomy, below the conjunctiva; the densely fibrous tarsal plate contains sebaceous glands (meibomian glands), H&E × 100.

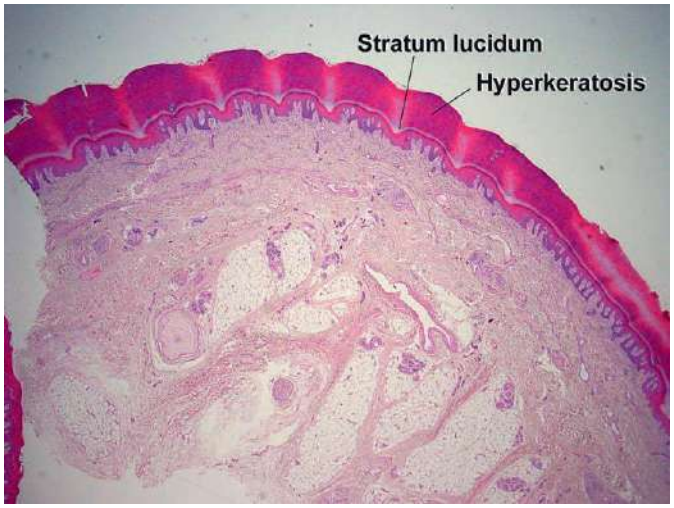

Fig. 1.15 Volar skin demonstrates a thick stratum corneum and lack of hair follicles, low power, H&E × 40.

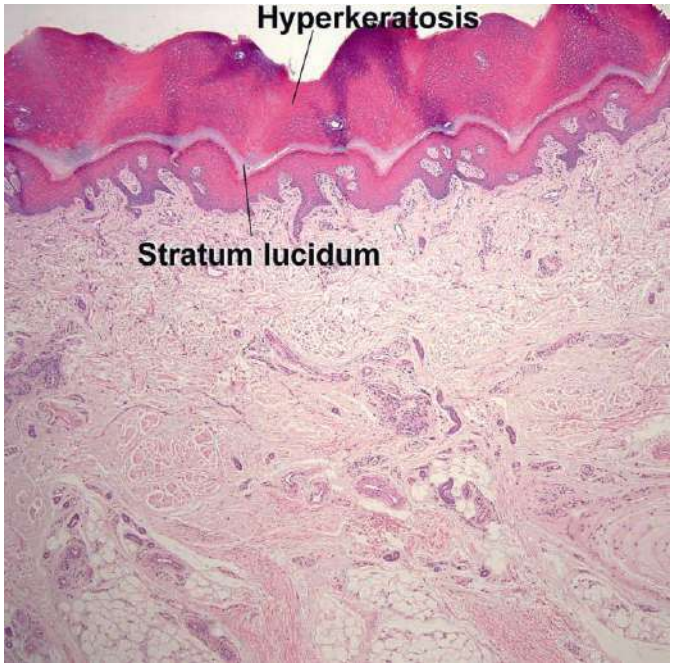

Fig. 1.16 Volar skin demonstrating a thick corneum and dermis, H&E × 100.

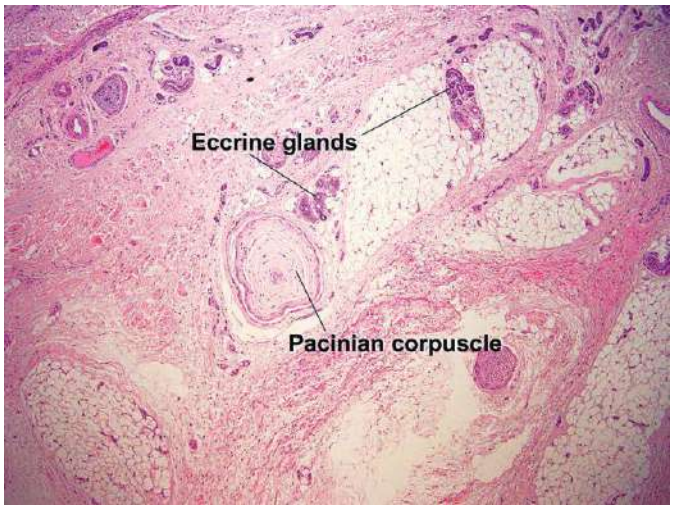

Fig. 1.17 Volar skin, with deep tissue demonstrating Pacinian corpuscles, H&E × 100.

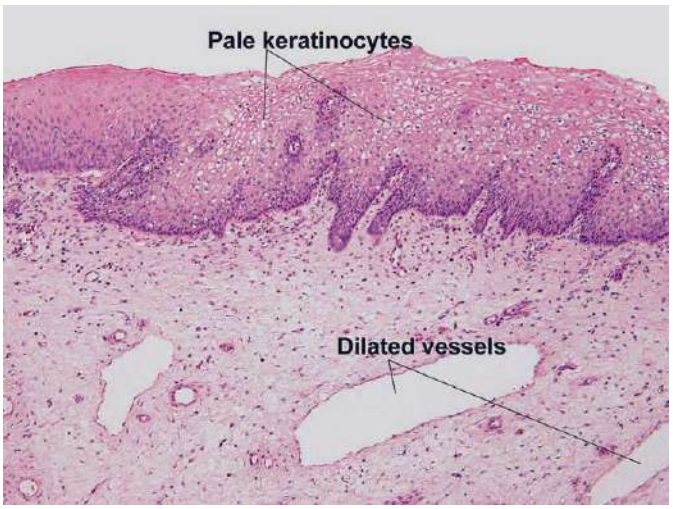

Fig. 1.18 Mucosal surface demonstrating nonkeratinizing epithelium and submucosa, H&E × 200.

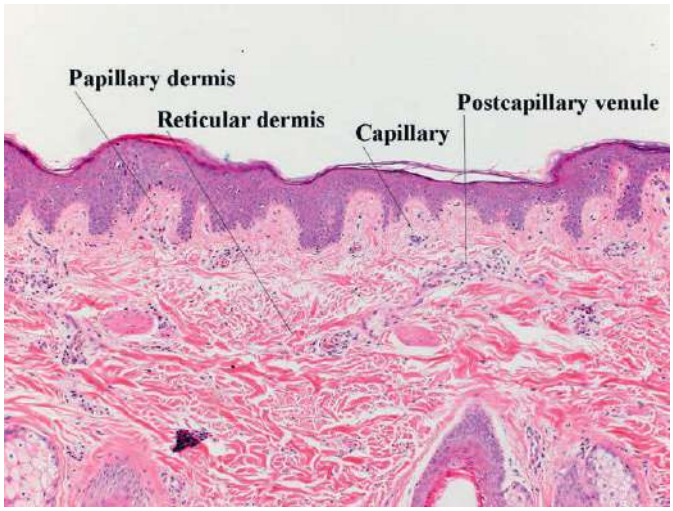

Fig. 1.19 Below the epidermis, the papillary dermis is composed of fine, nonbundled collagen. Capillaries are present within the papillary dermis, and the postcapillary venule sits at the junction of the papillary and reticular dermis. H&E × 40.

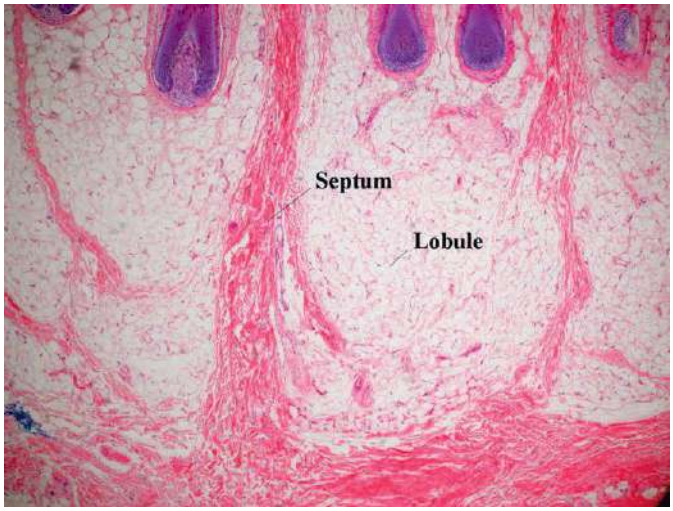

Fig. 1.20 The lobules of the subcutaneous fat are separated by fibrous septae. H&E × 40.

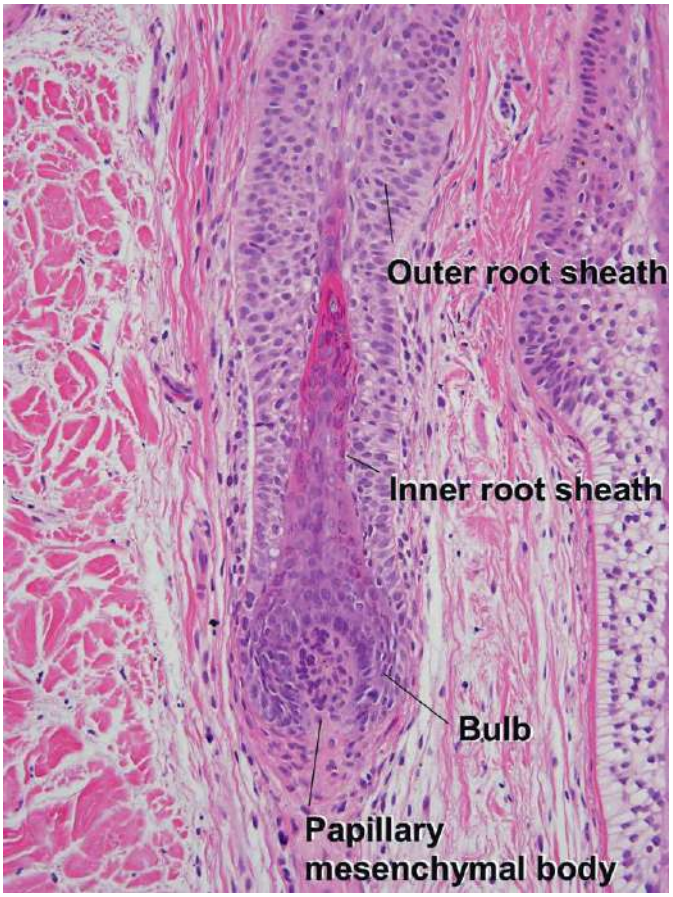

Fig. 1.21 Hair anatomy, vertical, H&E × 200.

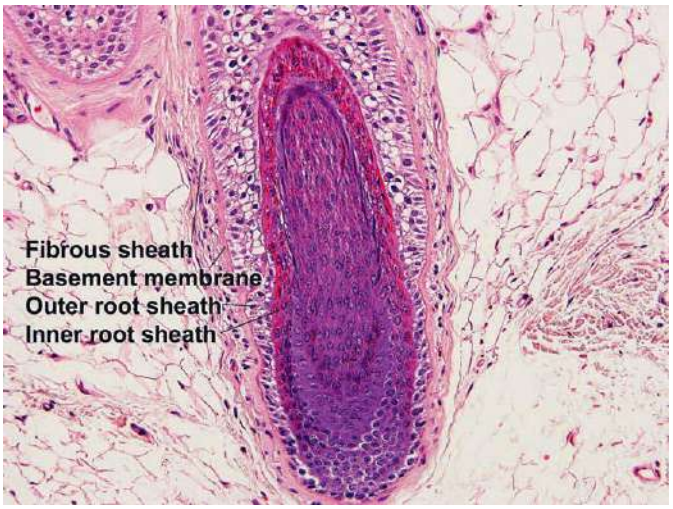

Fig. 1.22 In the inferior segment, the hair bulb gives rise to the inner and outer root sheath, H&E × 200.

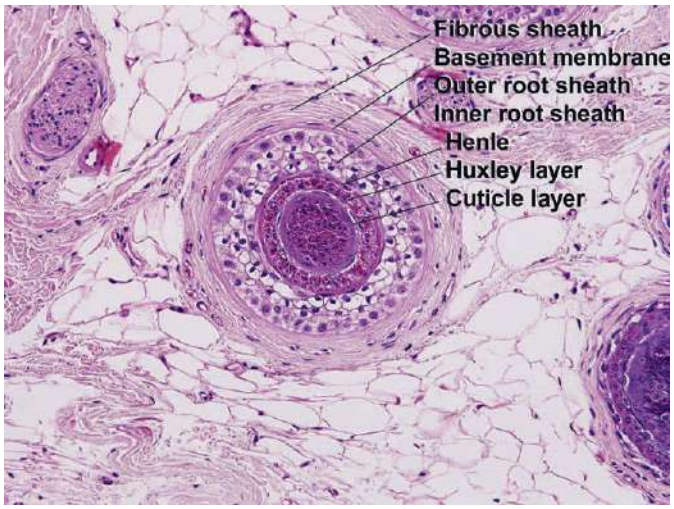

Fig. 1.23 Hair anatomy, transverse, H&E × 200.

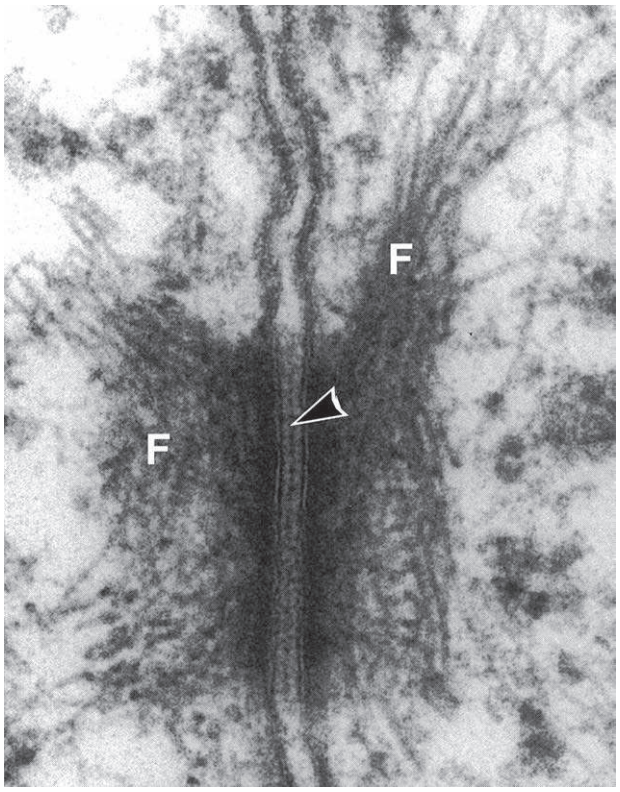

Fig. 1.24 Desmosome: A classic desmosome showing the following features: (1) Uniform gap of 20 to 30 nm between the apposed trilaminar plasma membranes with an intermediate line (*arrow*) in this gap. (2) Sharply delineated dense plaques into which tonofibrils (F) converge. *Courtesy Sunita Bhuta, MD.*

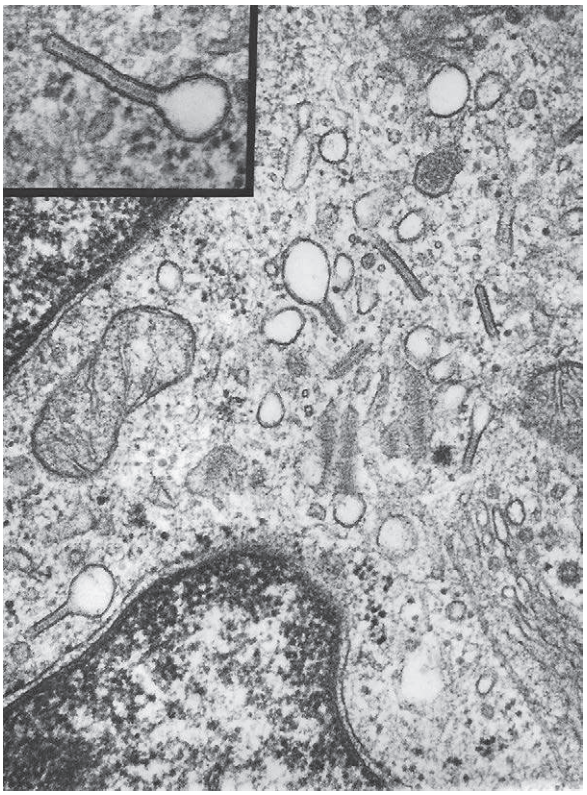

Fig. 1.25 Langerhans cell with Birbeck granules. This electromicrograph shows characteristic racket-shaped profiles of the granules in the cytoplasm (*inset* with higher magnification of the Birbeck granule). *Courtesy Sunita Bhuta, MD.*

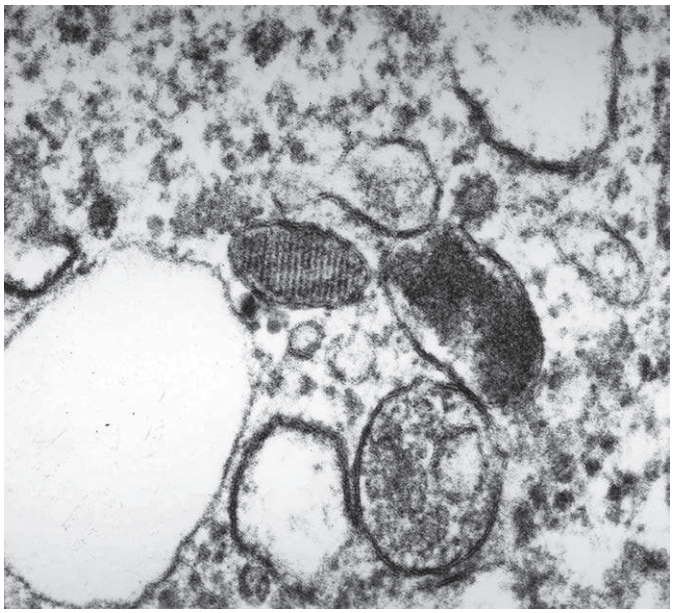

Fig. 1.26 Premelanosome: Solitary melanosome with characteristic internal striated structure. *Courtesy Sunita Bhuta, MD.*

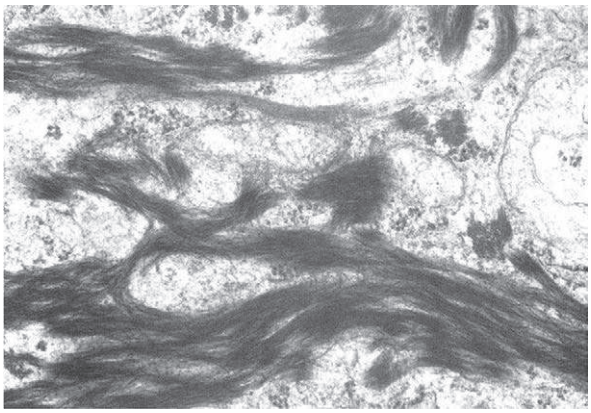

Fig. 1.27 Tonofibrils: Tonofibrils (intermediate filaments) lying free in the cytoplasm of a squamous cell. *Courtesy Sunita Bhuta, MD.*

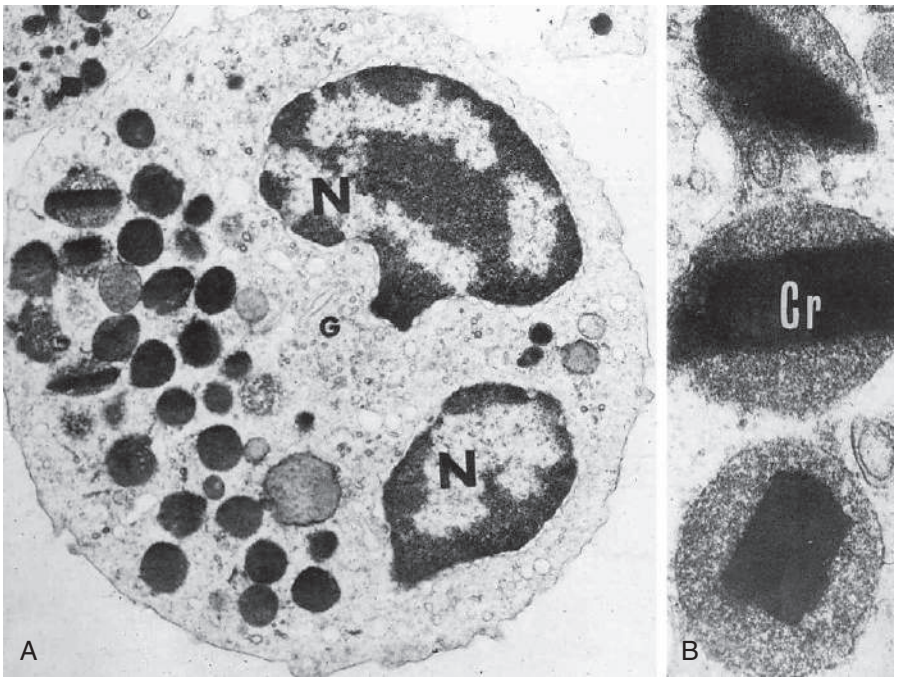

Fig. 1.28 Eosinophil: (A) Binucleate (N) with intracytoplasmic specific granules. (B) Specific granules have a finely granular matrix and a crystalline core. *Courtesy Sunita Bhuta, MD.*

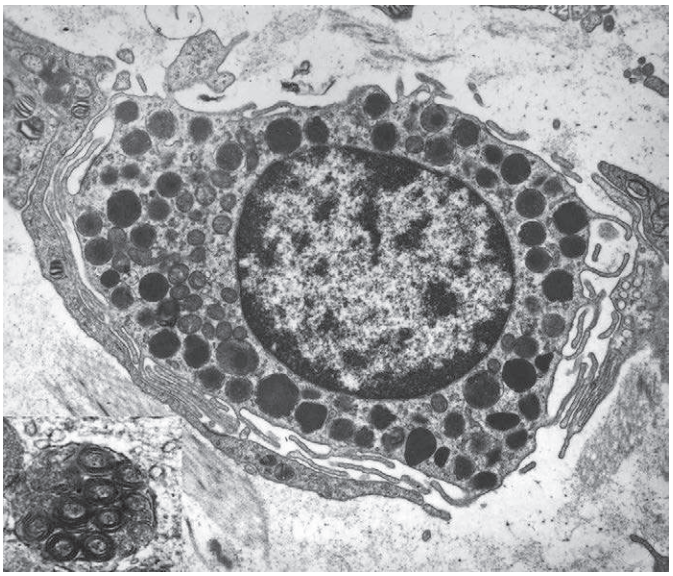

Fig. 1.29 Mast cell: Mast cell with numerous electron-dense granules. The inset shows internal structure of granules with membranous whorls (scrolls). *Courtesy Sunita Bhuta, MD.*

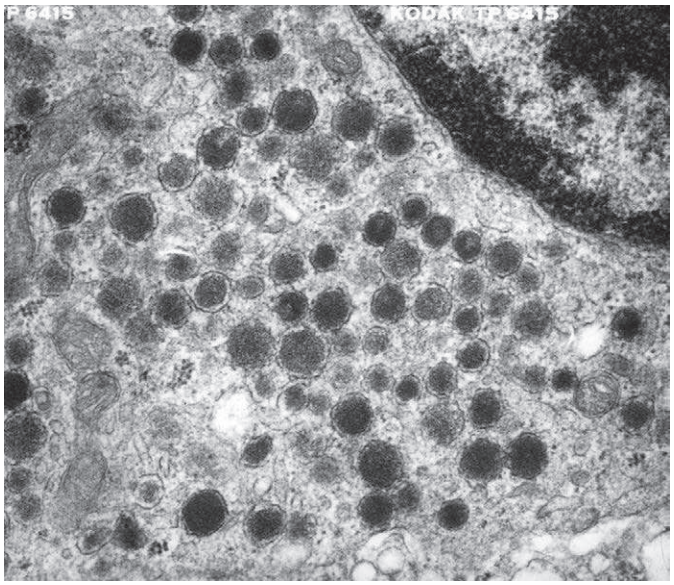

Fig. 1.30 Merkel cell: Merkel cell with intracytoplasmic membrane bound, electron-dense granules with a halo (neurosecretory granules). *Courtesy Sunita Bhuta, MD.*

Fig. 1.31 Skin tension lines relate to creases visible in older skin. They relate to passive skin tension, as well as active contraction of superficial muscular aponeurotic system muscle. Optimal surgical results can be achieved by aligning incisions along these lines.

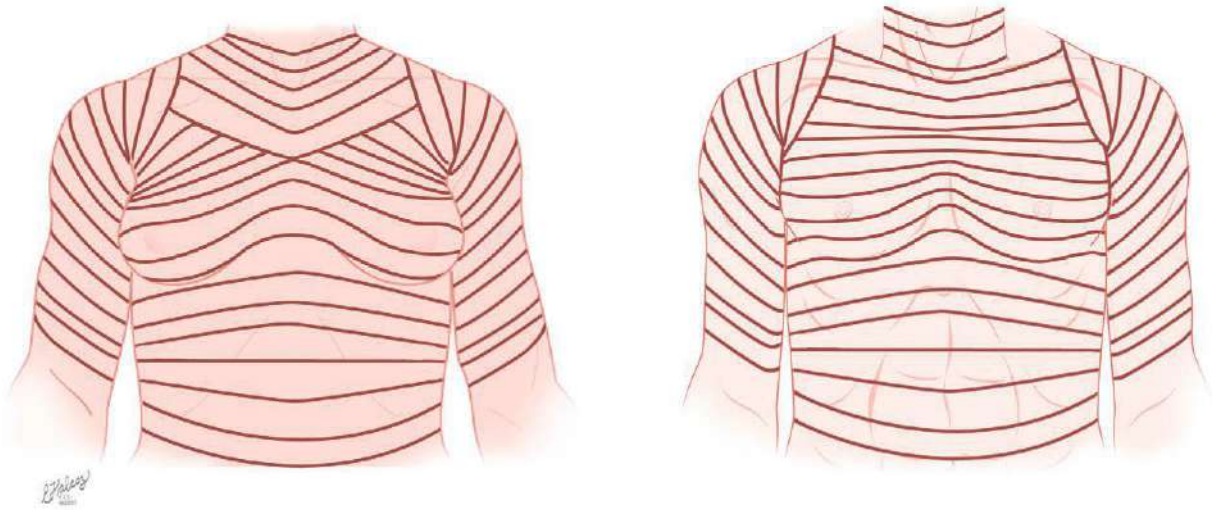

Fig. 1.32 Skin tension lines on the trunk.

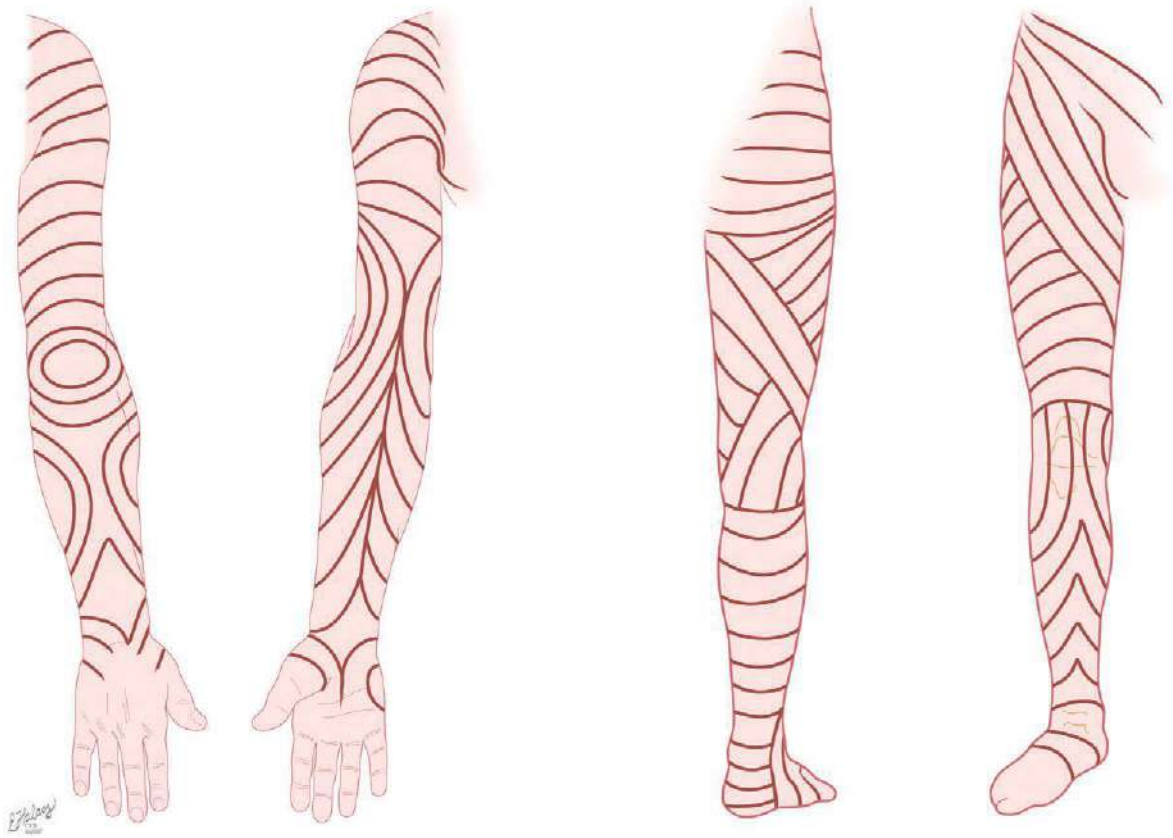

Fig. 1.33 Skin tension lines on the extremities.

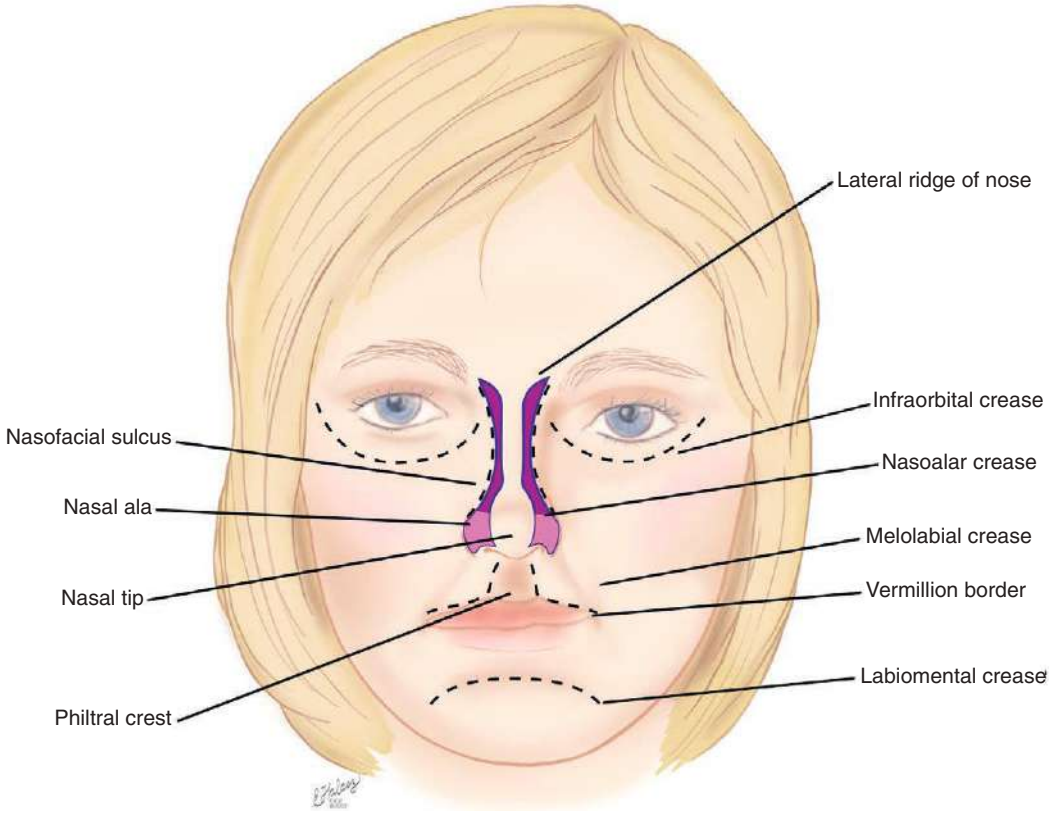

Fig. 1.34 Major anatomic landmarks.

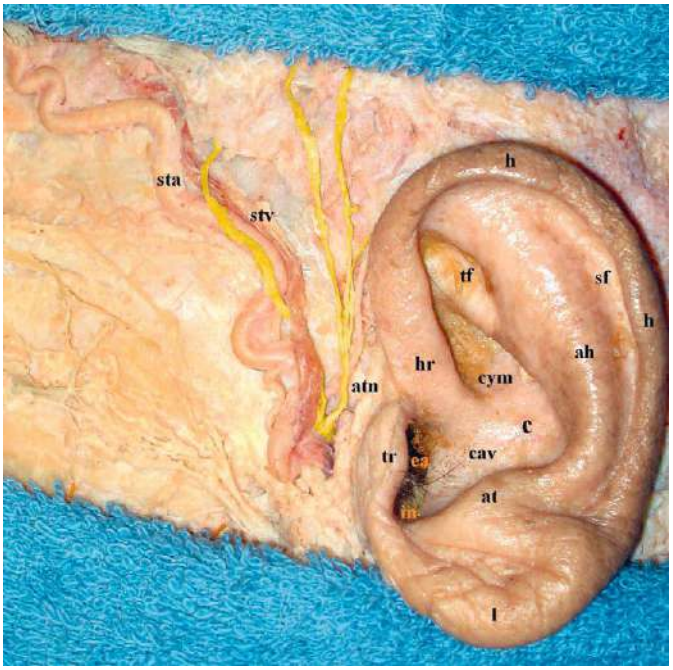

Fig. 1.35 Anatomy of the ear, superficial temporal artery, and auriculotemporal nerve. *Courtesy Joseph F. Greco, MD, and Christopher Skvarka, MD.*

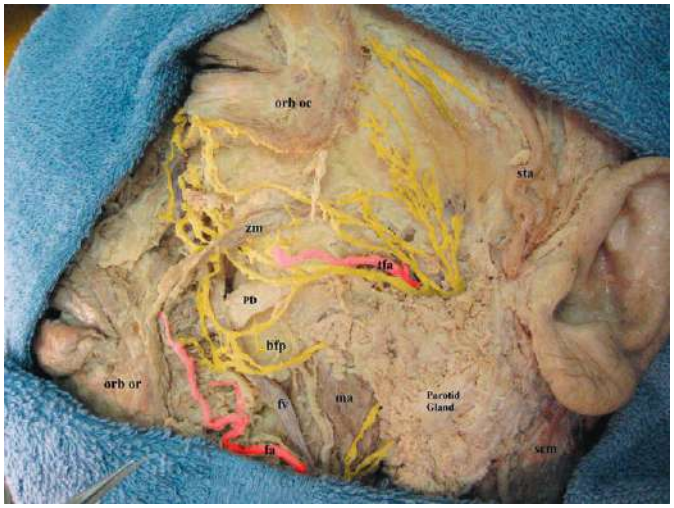

Fig. 1.36 Anatomy of the parotid gland and related structures. *Courtesy Joseph F. Greco, MD, and Christopher Skvarka, MD.*

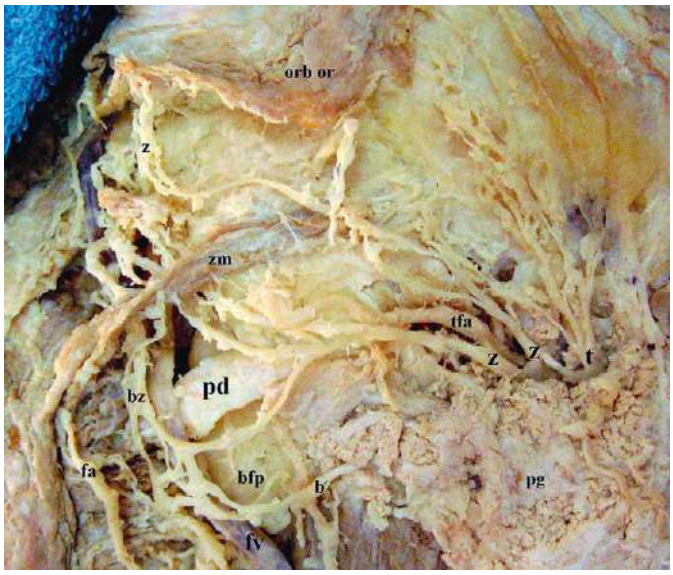

Fig. 1.37 Anatomy of the parotid duct and facial nerve. *Courtesy Joseph F. Greco, MD, and Christopher Skvarka, MD.*

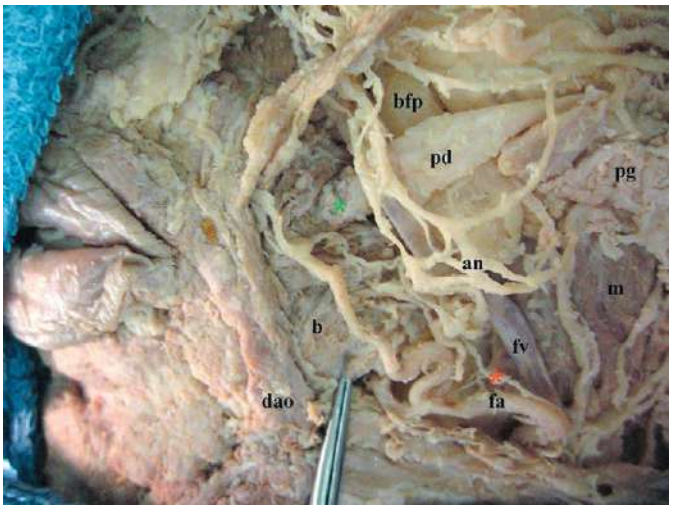

Fig. 1.38 Parotid duct as it pierces the buccinators muscle. *Courtesy Joseph F. Greco, MD, and Christopher Skvarka, MD.*

Fig. 1.39 Superficial muscular aponeurotic system. *Courtesy Joseph F. Greco, MD, and Christopher Skvarka, MD.*

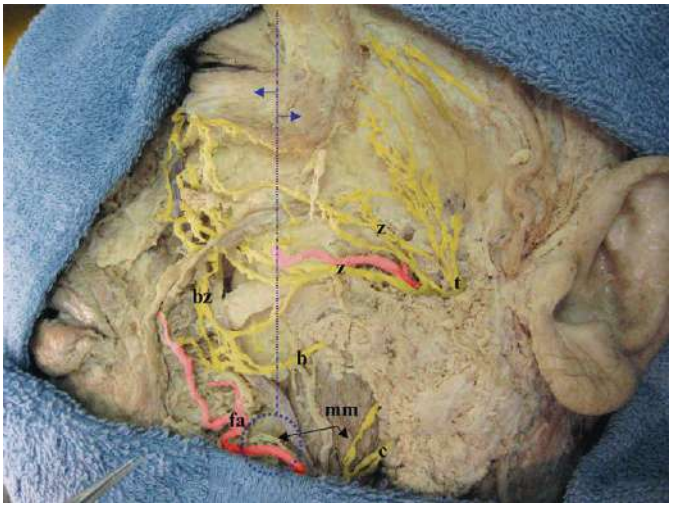

Fig. 1.40 Anatomy of the facial nerve. *Courtesy Joseph F. Greco, MD, and Christopher Skvarka, MD.*

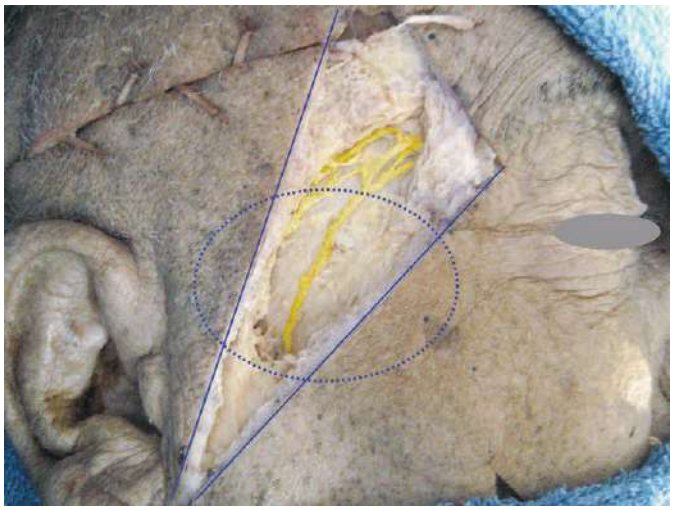

Fig. 1.41 The facial nerve: Danger zone for dermatologic surgery. *Courtesy Joseph F. Greco, MD, and Christopher Skvarka, MD.*

Fig. 1.42 Muscles of facial expression. *Courtesy Joseph F. Greco, MD, and Christopher Skvarka, MD.*

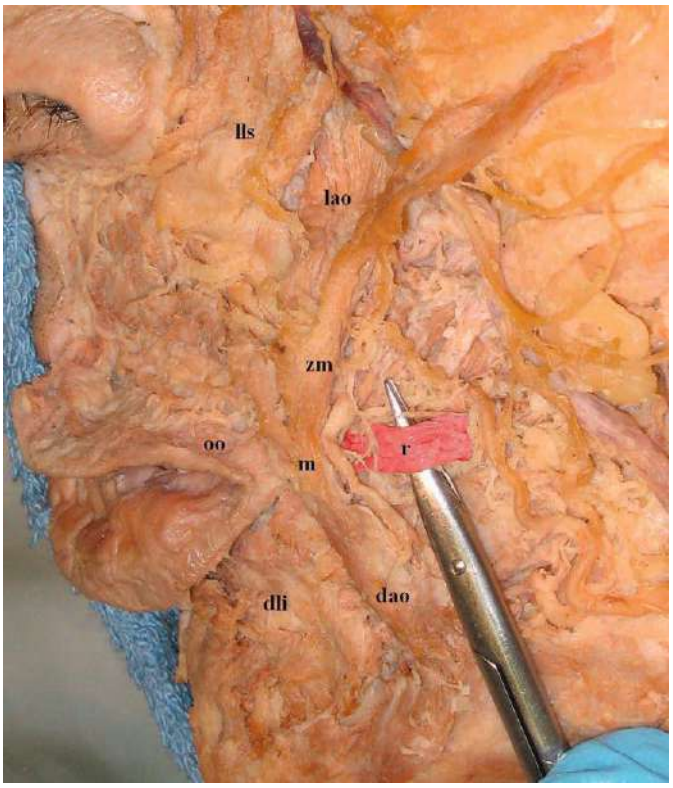

Fig. 1.43 Modiolus, elevators, and depressors. *Courtesy Joseph F. Greco, MD, and Christopher Skvarka, MD.*

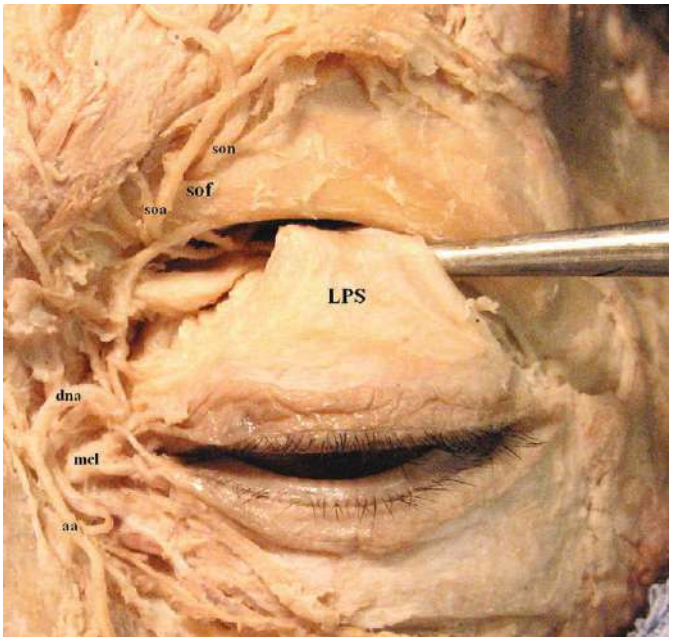

Fig. 1.45 Levator palpebrae superioris. *Courtesy Joseph F. Greco, MD, and Christopher Skvarka, MD.*

Fig. 1.44 Innervation of the facial skin. *Courtesy Joseph F. Greco, MD, and Christopher Skvarka, MD.*

Fig. 1.46 Medial forehead: Supraorbital and supratrochlear neurovascular structures. *Courtesy Joseph F. Greco, MD, and Christopher Skvarka, MD.*

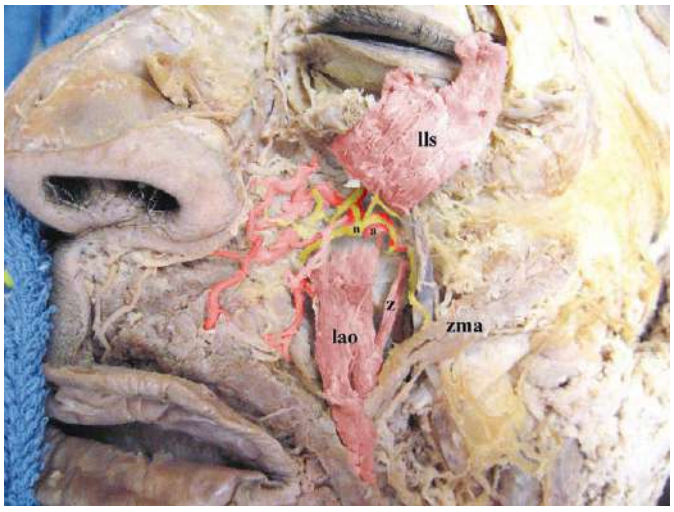

Fig. 1.47 Infraorbital foramen and related structures. *Courtesy Joseph F. Greco, MD, and Christopher Skvarka, MD.*

Fig. 1.48 Mental foramen and related structures. *Courtesy Joseph F. Greco, MD, and Christopher Skvarka, MD.*

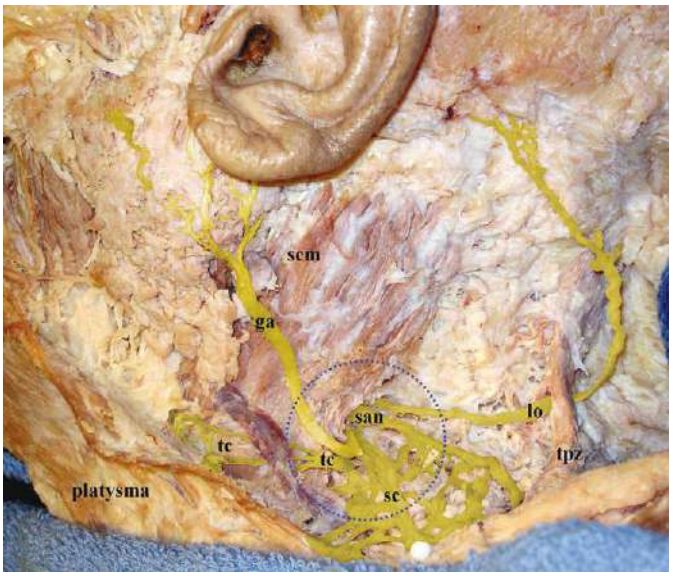

Fig. 1.49 Anatomy of the posterior triangle of the neck (Erb point). *Courtesy Joseph F. Greco, MD, and Christopher Skvarka, MD.*

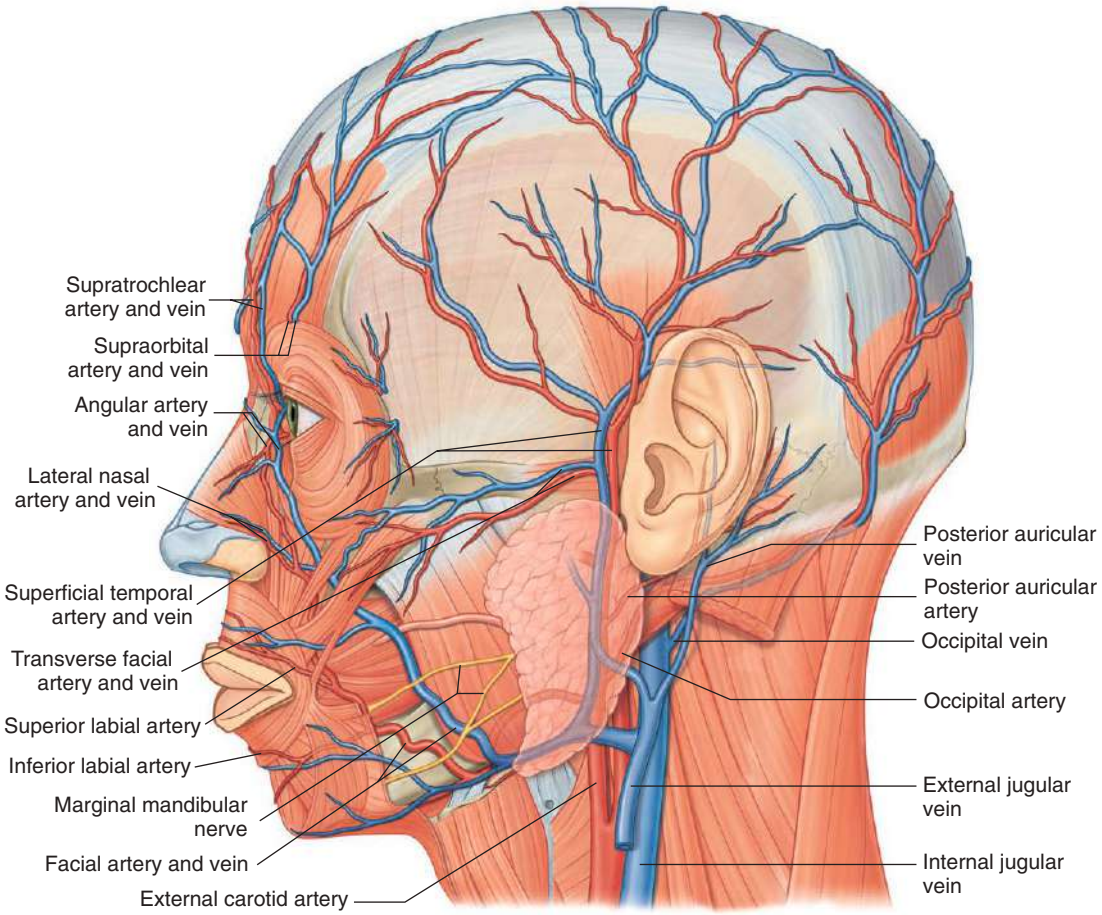

Fig. 1.50 Arterial and venous supply of the face.

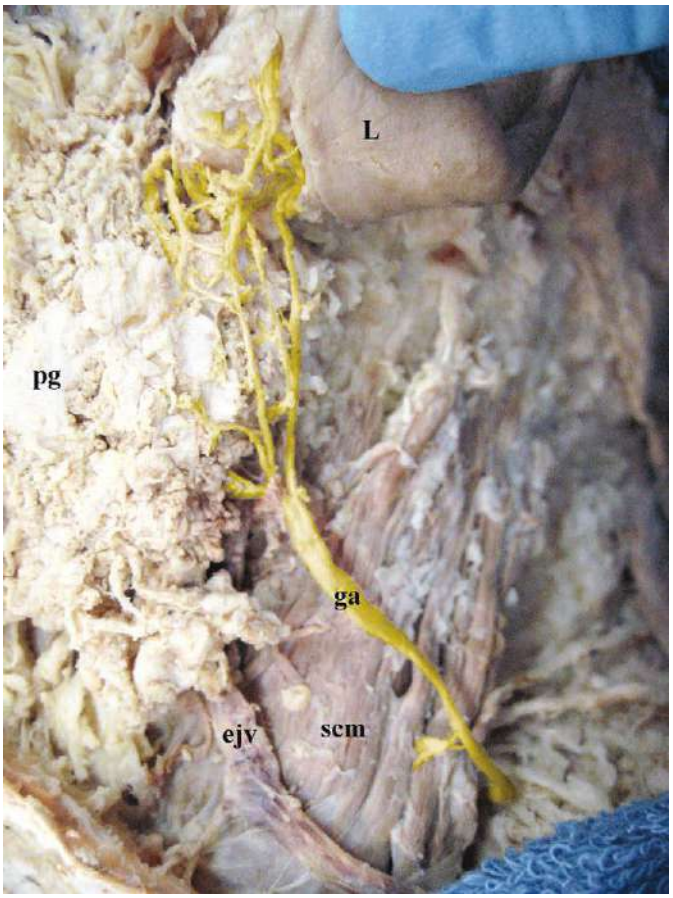

Fig. 1.51 Great auricular nerve and external jugular vein. *Courtesy Joseph F. Greco, MD, and Christopher Skvarka, MD.*

Fig. 1.52 Facial artery with angular artery. *Courtesy Joseph F. Greco, MD, and Christopher Skvarka, MD.*

Fig. 1.53 Inferior labial artery and related structures of the lower lip and chin. *Courtesy Joseph F. Greco, MD, and Christopher Skvarka, MD.*

Fig. 1.54 Superior labial artery and related structures of the upper lip and cheek. *Courtesy Joseph F. Greco, MD, and Christopher Skvarka, MD.*

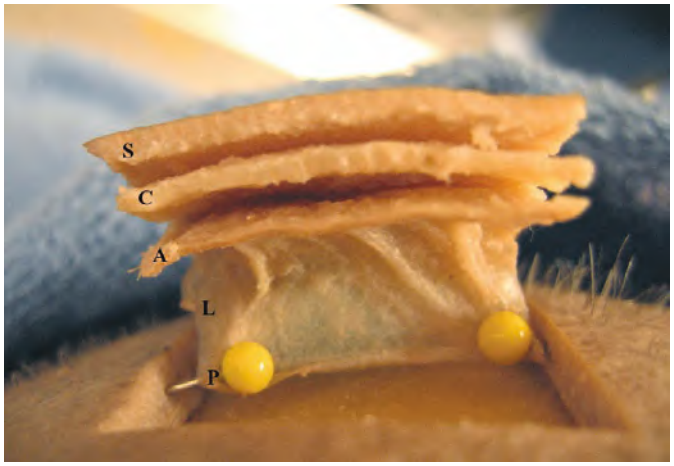

Fig. 1.55 Layers of the scalp. *Courtesy Joseph F. Greco, MD, and Christopher Skvarka, MD.*